

Differential utilisation of dissolved organic matter compound fractions by different biofilter microbial communities

Marta Vignola ^{a,*†}, Jeanine Lenselink^{a,†}, Dominic Quinn^a, Umer Zeeshan Ijaz ^a, Ryan Pereira ^b, William T. Sloan ^a, Stephanie Connelly ^a, Graeme Moore^c, Caroline Gauchotte-Lindsay ^a and Cindy J. Smith  ^a

^a James Watt School of Engineering, University of Glasgow, Glasgow G12 8LT, United Kingdom

^b The Lyell Centre, Heriot-Watt University, Edinburgh EH14 4AP, United Kingdom

^c Scottish Water, 6 Castle Drive, Dunfermline KY11 8GG, United Kingdom

*Corresponding author. E-mail: marta.vignola@glasgow.ac.uk

†Joint first author.

 MV, 0000-0002-3457-5748; UZI, 0000-0001-5780-8551; RP, 0000-0001-6492-7874; WTS, 0000-0002-9450-7384; SC, 0000-0001-5261-2090; CG-L, 0000-0002-4970-5031; CJS, 0000-0003-4905-0730

ABSTRACT

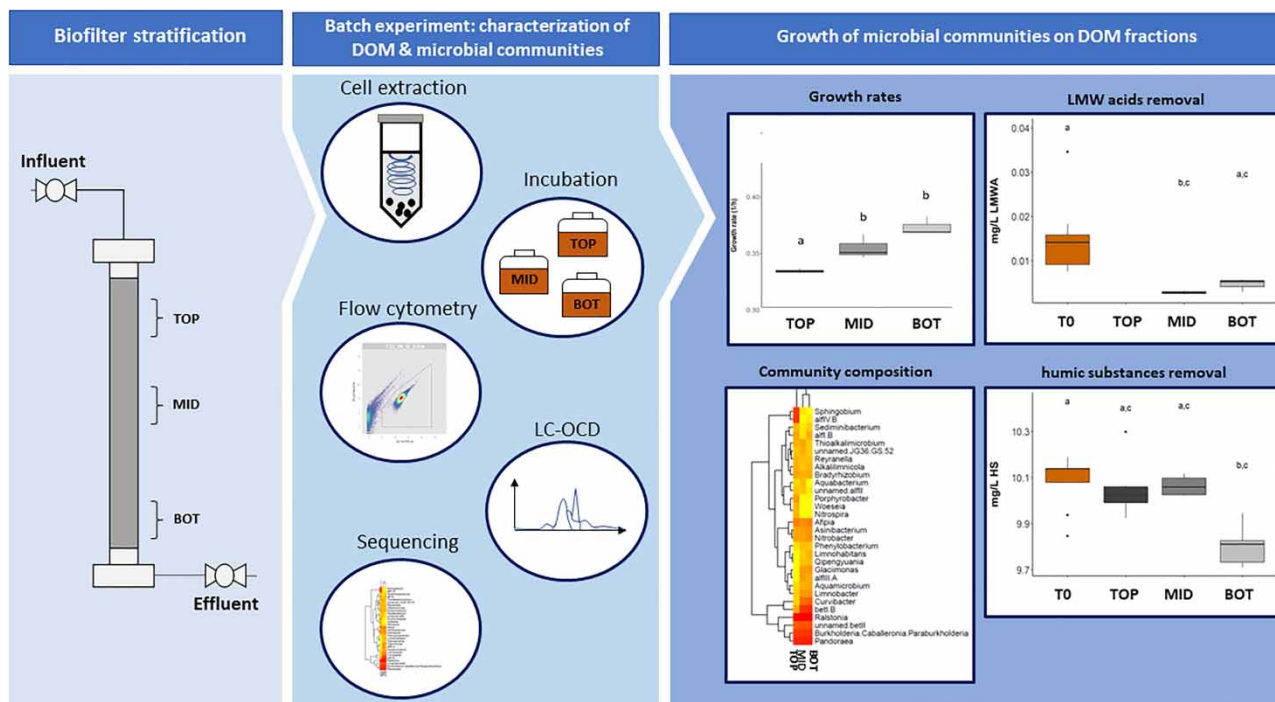
Dissolved organic matter (DOM) is a complex mixture of carbon-based compounds present in natural aquatic systems, which significantly affects drinking water treatment processes. Biofiltration, utilising biologically active beds of porous medium, offers a low-energy and low-chemical solution for controlling bioavailable DOM. However, the impact of microbial community composition on DOM degradation in biofilters remains poorly understood. This study aimed to explore the abilities of microbial communities from the top, middle, and bottom (TOP, MID, and BOT) of a biofilter to process DOM. We showed varying growth rates on the DOM, with bottom community exhibiting the highest cell abundance at the end of the experiment ($1.83 \times 10^6 \pm 9 \times 10^3$; $2.06 \times 10^6 \pm 1 \times 10^4$; $2.15 \times 10^6 \pm 7 \times 10^3$ cells/mL for the TOP, MID, and BOT, respectively). The three communities showed different preferences for utilising specific DOM fractions, with the bottom community targeting more complex ones. The microbial communities from the bottom of the biofilter had a higher relative abundance of the *Curvibacter* genus, suggesting it could play a crucial role in degrading complex DOM fractions. These findings highlight the influence of microbial community composition on DOM degradation in biofilters, providing valuable insights for optimising their performance.

Key words: biofiltration, community assembly, dissolved organic matter, LC-OCD, microbial degradation

HIGHLIGHTS

- Communities were extracted from three different depths of a biofilter (TOP, MID, and BOT).
- Communities differed in growth kinetics, with BOT showing the greatest growth.
- The TOP and MID communities preferentially used the smaller fractions of DOM.
- The BOT community used the more complex DOM fraction of humic substances.
- Microbial communities from different depths of a biofilter exhibit distinct abilities to degrade DOM.

GRAPHICAL ABSTRACT



INTRODUCTION

Dissolved organic matter (DOM) is a heterogeneous blend of carbon-based compounds ubiquitous in natural aquatic systems such as surface waters and deep or shallow groundwater, many of which serve as sources of drinking water (Leenheer & Croué 2003). DOM is a complex mixture of proteins, carbohydrates, humic substances, and other molecules, which must be significantly reduced during water treatment to provide potable water. This can be challenging as DOM composition and concentration in freshwater can significantly impact the efficacy of treatment in a drinking water treatment plant (DWTP) as well as the quality of the potable water produced (Matilainen *et al.* 2011; Terry & Summers 2018). DOM is the main precursor of carcinogenic disinfection by-products (Gang *et al.* 2003), and the prime contributor to regrowth of heterotrophic bacteria in the distribution network (Prévost *et al.* 1998). Therefore, the effective reduction of DOM levels in the source water, prior to disinfection and distribution, is essential to produce safe and high-quality drinking water.

Biofiltration, the process whereby water is passed through a biologically active bed of porous medium, is a very appealing technology for the control of bioavailable DOM in DWTPs as it is characterised by low-energy requirements, low chemical consumption, and ease of construction (Urfer *et al.* 1997; Basu *et al.* 2016). As such biofiltration is an ideal sustainable solution for DOM reduction and understanding the key biological mechanisms underpinning the process could further enhance its performance.

Several studies have started to investigate the transformation and the removal of different DOM fractions through a DWTP (Baghoth *et al.* 2011; Lautenschlager *et al.* 2014) and in biofiltration processes (Boon *et al.* 2011; Chen *et al.* 2016; Peleato *et al.* 2016; Moona *et al.* 2021). These studies have shown that biofilters are generally effective in removing labile and highly bioavailable fractions of DOM. However, the removal efficiency of the more recalcitrant DOM fractions varied across the types of biofilter investigated (Peleato *et al.* 2016; Moona *et al.* 2021). In some cases, authors speculated that these differences could be attributed to variations in the composition of the microbial communities inhabiting the biofilters (Peleato *et al.* 2016). While there has been much focus on the composition of biofilter communities (Lautenschlager *et al.* 2014; Palomo *et al.* 2016; Oh *et al.* 2018; Hu *et al.* 2020) through depth, and work towards linking their key role in the treatment process (Pinto *et al.* 2012; Bai *et al.* 2013), there remains a knowledge gap on the link between microbial community structure and function. This is particularly true in relation to the processing of DOM fractions and on understanding the underlying ecological mechanisms that drive community assembly and structure in a filter.

While this link, between microbial community structure and the degradation of DOM fractions, in biofilters is a relatively poorly explored area, in recent years, there have been several published studies examining this topic in various other natural environments, including marine (Cottrell & Kirchman 2000; Rocker *et al.* 2012; Chen *et al.* 2022), coastal (Broman *et al.* 2019), sediment (Wu *et al.* 2018) and freshwater (Logue *et al.* 2016). Notably, Logue *et al.* (2016) were able to successfully demonstrate a direct link between microbial communities' composition in freshwater environments and their ability to degrade different DOM fractions. Yet, in biofilters, despite being a key process for the removal of DOM only a few studies to date have focused on DOM fractions removal and associated microbial community composition within biofilters (Boon *et al.* 2011; Lautenschlager *et al.* 2014). One of these studies by Boon *et al.* (2011) identified gradients of nutrient concentrations through a granular activated carbon (GAC) biofilter as a driver for the establishment of different environmental niches at the different depths of the filter bed which, in turn, selected communities differing in their composition. Furthermore, they were able to associate different DOM removal efficiencies with communities present at different filter depths, with the communities in the lower filter sections showing the highest removal efficiencies. The authors suggested that the different functionalities shown by the communities at different biofilter sections could be the result of their different structures, concluding that microbial community composition drives biological DOM removal efficiencies in a biofilter. What is still unknown is how the composition of the communities colonising different depths of a biofilter affect their ability to degrade different fractions of DOM and how this impacts their growth patterns.

In this study, we further explore the ability of communities from different depths of a biofilter to process DOM. Specifically, we asked if different microbial communities, collected from various depths within a biofilter, degraded different fractions of the DOM in the water. We hypothesised that, as the water flows through the filter, the microbial communities and the fraction of DOM they use to support growth at a given depth of the filter are intimately linked with processes happening above, analogously to the river continuum concept theory developed by Vannote *et al.* (1980). Similarly, to what happens in a river, the communities at the top of the filter receive water rich in heterogeneous assemblages of labile and refractory DOM. These communities have the luxury of choosing which compounds to use; the labile compounds are used first, as also observed by Wu *et al.* (2018) while the more refractory compounds are left in the stream for use by the communities at the bottom. Hence, the communities at the bottom of the filter are forced to adapt and survive on what is left, resulting in the enrichment of microorganisms capable of growing on more complex DOM compounds. This should result in a stratification of the composition of filter communities as well as a stratification of their ability to process the different DOM fractions.

To test our hypothesis, we conducted a batch experiment where bacterial communities extracted from the top, middle, and bottom sections of a laboratory-scale biofilter were inoculated with DOM within raw surface water. Communities' growth and the transformation of DOM were measured over time using Flow cytometry and Liquid Chromatography techniques. By employing this approach, we were able to study the growth patterns of the different bacterial communities and their abilities to degrade specific DOM fractions, providing insights into the processes occurring within the biofilter.

METHODS

Biofilter and water collection

Three 90-cm laboratory-scale GAC filters were operated for 12 weeks in a down-flow mode. Water for the experiment was collected from Pateshill Water Treatment Works, Scottish Water (hereafter called freshwater), and filtered on site through 10- μ m polypropylene cartridge filters and stored in plastic jerrycans at room temperature prior to its use. A schematic representation of the filters is shown in Figure 1; operational parameters are presented in Table 1.

Glassware preparation

All glasswares were prepared following the protocol of Hammes & Egli (2005) to reduce the Available Organic Carbon (AOC) contamination. In short, all glasswares and screw caps were washed with a common detergent and rinsed three times in 18.2 M Ohm deionised carbon-free water (Milli-Q) water and then submerged overnight in 0.2 M HCl and again rinsed three times with Milli-Q water. Borosilicate vials were subsequently heated in a Muffle oven to 550 °C for at least 6 h.

AOC-free inocula preparation

Three *inocula* (TOP, MID, and BOT) were created starting from the biofilters replicates at the end of the 12-week period: 500 mg of GAC was collected from each section of the first 10 cm of the filter at 0–2, 2–4, 4–6, 6–8, 8–10 cm depths, and

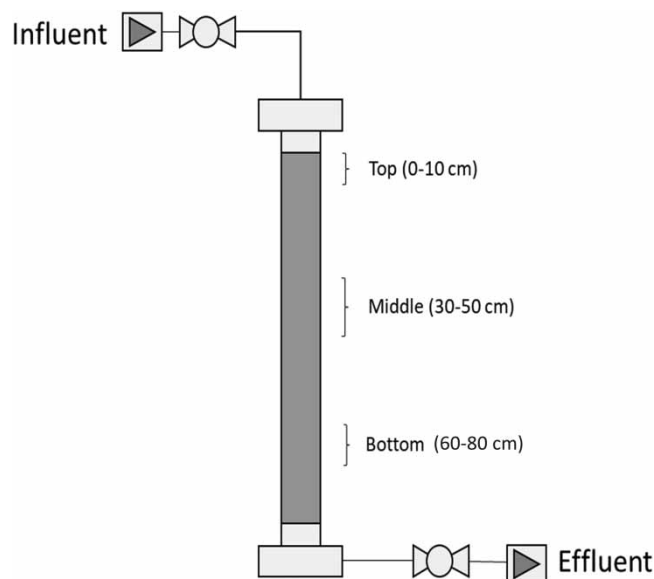


Figure 1 | Schematic representation biofilter.

Table 1 | GAC filter and water quality parameters

GAC depth	cm	90
Column diameter	cm	2.6
Filter volume	cm ³	478
GAC apparent density	Kg/m ²	500
GAC type	–	Norit [®] GAC 1240 W
Flowrate	mL/min	1.06
Empty bed contact time	h	7.5
Run period	h	1,968
DOC IN	mg/L	11.4 ± 1.4
pH	–	8.0 ± 0.1
Conductivity	S/m	118.0 ± 3.9
Temperature	°C	22 °C

transferred to sterile 5-mL containers (TOP); 2,500 mg of GAC was collected in sterile 5-mL containers from 30–50 cm (MID) and 60–80 cm depths (BOT). 3 mL of filtered (0.22 µm filter) Milli-Q water was added to all the GAC samples and vortexed for 5 s to detach biofilm. A higher GAC to Milli-Q water ratio was chosen for the MID and BOT sections to take into account lower biomass concentration. 500 µL were withdrawn from each of the five extractions of 0–10 cm and combined, while 1 mL was withdrawn from the 30–50 and 60–80 samples. This procedure was repeated for each of the three biofilters; extracts of the same depth (0–10, 30–50, or 60–80) from the three reactors were pooled together in 15-mL sterile polypropylene tubes stored in the dark at 4 °C and used within 4 h to prepare three (TOP, MID, and BOT) AOC-free *inocula* as described in Hammes & Egli (2005). For this, 200 µL from each pooled extract was added to 50-mL filtered (0.1 µm, Millex-GP, Millipore) freshwater in 100-mL AOC-free borosilicate vials. Vials were incubated without further amendments at 30 °C for 14 days. At the end of the 14 days of incubation, the content of the vials was transferred to 50-mL sterile polypropylene centrifuge tubes. The cells were harvested by centrifugation (10 min, 3,000 g), resuspended in Milli-Q water amended with a mineral buffer, as described by LeChevallier *et al.* (1993) and then poured into fresh 100-mL AOC-free borosilicate vials. Finally, the vials were incubated for a further 7 days to ensure that all residual organic was depleted. *Inocula* were kept in the dark and at 4 °C until their use for the following experiment.

Experimental set-up

The experiment was performed applying a batch culture approach in which the same filtered fresh water was inoculated independently with each of the three AOC-free *inocula* (TOP, MID and BOT); cell growth and associated degradation of DOM were measured as described below. Also, DNA was extracted for further 16S rRNA gene sequencing.

Cell abundance and specific growth rate

For cell abundance, 100-mL AOC-free glass vials, sealed with Teflon-coated screw caps (Fisherbrand™ with PTFE liner material) were prepared in triplicate. Vials were filled with 60 mL of 0.1- μm filtered freshwater (0.1 μm , Merck™ Stericup™) to remove autochthonous microorganisms. Water was inoculated with either TOP, MID, or BOT *inoculum* to a similar concentration of cells ($4.35 \times 10^5 + -2 \times 10^2$ cells/mL). Alongside the three experimental treatments, a negative control, filtered fresh water only with no added *inocula*, was incubated. All the vials were incubated at 30 °C, in the dark. Samples were collected from triplicates at 0, 10, 12, 14, 16, 18, 20, 22, 23, 36 h (negative controls were measured at 0 and 23 h only). At each timepoint, vials were opened, and 1 mL of sample was withdrawn using a sterile pipette; the samples were immediately fixed with 1 mL of 1% v/v Glutaraldehyde, stored at 4 °C in the dark and measured within 2 h by flow cytometry using a BD Accuri C6 Plus flow cytometer equipped with a laser emitting at 488 nm (66 $\mu\text{L min}^{-1}$ flowrate; 50 μL sample analysed). Samples (1 mL) were stained with 10 $\mu\text{L/mL}$ SYBR Green I (1:100 dilution in Tris-EDTA buffer solution, pH 8.0) and incubated in the dark at 37 °C for at least 13 min before measurement (Hammes *et al.* 2008; Vignola *et al.* 2018).

The specific growth in each sample was determined as follows:

$$\mu = \frac{(\ln(x_{T18}) - \ln(x_{T10}))}{\Delta t}$$

where x_{T18} and x_{T10} are the concentrations measured after 18 and 10 h of incubation and Δt is the time interval between the two points.

DNA extraction and 16S rRNA gene sequencing

At the end of the 36 h of incubation, replicates from each depth treatment (TOP, MID, or BOT) were pooled, and cells filtered onto 0.2- μm membrane filters (Whatmann) and frozen at -80 °C until DNA extraction. DNA was extracted with the FastDNA Spin Kit for soil kit (MP Biomedicals) following the manufacturer's protocol. Extracted DNA was quantified using the Qubit dsDNA HS Assay Kit (Life Technologies, Eugene, OR, United States) with a Qubit fluorometer (Invitrogen, Eugene, OR, United States). V3-V4 regions of 16S rRNA gene was amplified for sequencing using the Illumina MiSeq (at GENEWIZ, Inc, South Plainfield, NJ, USA) (details are given in Supplementary material).

16S rRNA gene sequencing analyses

Raw sequence data were analysed using QIIME2 pipeline and Deblur algorithm (Caporaso *et al.* 2010). The Deblur algorithm was used to facilitate better discrimination as it is an overlap free algorithm allowing only one set of reads, either forward or reverse reads. The reverse reads were of low quality and therefore were discarded from the analyses. Additionally, while selecting trim length for Deblur, we have used https://qiita.ucsd.edu/static/doc/html/deblur_quality.html for their suggestions and as such reads were trimmed using the recommendations. The sequences were then trimmed above a Phred Quality score of 20 using qiime2. Amplicon sequence variants (ASVs) were produced using Deblur against SILVA v138 gene reference database. Qiime's align-to-tree-mafft-fasttree was then used to generate the rooted phylogenetic tree. The representative sequences were taxonomically classified using TaxAss workflow (<https://github.com/McMahonLab/TaxAss>) which uses an additional database formatted in the same format as SILVA v138 database to resolve ASVs that are not resolved by standard Naïve Bayesian Classifier using the standard database. The biom file for the ASVs was generated by combining the abundance table with taxonomy information using biom utility available in Qiime2 workflow.

Further analyses on the ASVs table were performed using R (version 4.0.2). Taxonomic alpha diversity indexes – Richness, Shannon and Fisher Alpha – were estimated after rarefying at the lowest sequencing depth of 53,948. These indexes are employed to describe the microbial biodiversity of the communities in terms of richness, as the number of different species present in the samples, and evenness as a distribution of species abundances. While Richness and Fisher Alpha indexes relate to richness only, Shannon relates to both. The abundance table was then normalised using TSS + CLR (Total Sum Scaling followed by Centred Log Ratio) normalisation at the Genus level as per recommendations by Rohart *et al.* (2017).

LC-OCD-UVD-OND sample preparation

DOM compound groups were analysed using liquid chromatography-organic carbon detection-ultraviolet detection-organic nitrogen detection (LC-OCD-UVD-OND Huber *et al.* 2011). For LC-OCD-UVD-OND analyses, 250 mL of AOC-free serum bottles were prepared as described above, with the ratio medium/headspace kept the same as the 100 mL glass vials. The amount of *inoculum* added was changed to have the same initial concentration of cells. Bottles were capped with metal crimp and silicone septa. All the vials were incubated at 30 °C, in the dark.

At T0, 50-mL medium was poured into a 60-mL carbon-free glass vial; at T23, incubated bottles were decapped, and 50-mL sample was poured into a 60-mL carbon-free glass vial. For the two time points, the samples were stored at room temperature in the dark, transported to the Lyell Centre, Edinburgh and measured (three technical replicates per sample) within 24 h.

The LC-OCD-UVD-OND separates DOM without prior modification by injecting ~1 mL of water onto a size exclusion column (SEC; 2 mL min⁻¹; HW50S, Tosoh, Japan) with a phosphate buffer (potassium dihydrogen phosphate 1.2 g L⁻¹ plus 2 g L⁻¹ di-sodium hydrogen phosphate × 2 H₂O, pH 6.58) to identify five different DOM classes. These classes include (i) biopolymers that are likely hydrophobic, high molecular weight (10,000 g mol⁻¹ or higher), largely non-UV-absorbing extracellular polymers with saturated structures, polysaccharides and some contribution of proteins or amino sugars; (Huber *et al.* 2011) (ii) ‘humic substances’ (HS; with higher molecular weight at ~1,000 g mol⁻¹ with UV-absorbing aromatic molecular aggregates of relatively small molecules, stabilised by the hydrophobic effect and hydrogen bonds); (Gerke 2018) (iii) ‘building blocks’ (BB) that are UV-absorbing humics of lower-molecular-weight (300–500 g mol⁻¹) that have been shown to include microbial breakdown products of HS; (Huber *et al.* 2011; Velten *et al.* 2011) (iv) low-molecular-weight ‘neutrals’ (LMWN; 350 g mol⁻¹) characterised as non-UV-absorbing, weakly or uncharged hydrophilic or amphiphilic compounds that can include alcohols, aldehydes, ketones, and amino acids hydrophilic; and (v) low-molecular-weight acids (LMWA; 350 g mol⁻¹). All carbon pools were quantified and molecularity (nominal molecular weight (NMW)) (Huber *et al.* 2011) given.

The limit of detection (LOD) of the OND and OCD were calculated as three times the standard deviation of the mean area of the noise for six blank injections (Milli-Q water), and the values were converted to concentration units using calibration curves. The limit of quantification (LOQ) was calculated as 10 times the standard deviation of the mean area of the noise for six blank injections. The LOD for OCD and OND were 82 ppb/C and 53 ppb/N, respectively. The corresponding LOQ were 273 ppb/C and 176 ppb/N, respectively. The reproducibility of the OCD and OND was tested by injecting 0.4 µg of International Humic Substances Society (IHSS) Humic Acid Standard (HS3S10H) in triplicate. For the OCD, the relative standard deviations (RSDs) were lower than 2.2%. For the OND, the RSDs of Humic Substances was lower than 1.6%.

Statistical analysis

All statistical analyses were carried out using R (version 4.0.2). For cell abundances and growth rates significant differences were ascertained by one-way analysis of variance (ANOVA) with data being normal and homogeneously distributed, followed by the Tukey *post hoc* test (equal variances, and equal group sizes) to discriminate between treatments with a 95% confidence level. For the LC-OCD-UVD-OND compound groups significant differences were ascertained by a Kruskal–Wallis *H* test as the data were not normally and homogeneously distributed, followed by the Dunn’s *post hoc* test (equal variances, unequal group sizes) to examine the pairwise comparison with *p*-values adjusted by the Bonferroni method. For both methods, the results were expressed by the mean for each group together with its variance (expressed by the standard error).

RESULTS

Increase in cell abundance

Over the course of the experiment, cell abundances increased in all three treatments (Figure 2(a)). Cell concentrations increased from an average of $4.35 \times 10^5 \pm 2 \times 10^2$ cells/mL at T0 for all three *inocula* ($n = 9$) to $1.83 \times 10^6 \pm 9 \times 10^5$ ($n = 2$ due to a problem with FCM analyses on one replicate); $2.06 \times 10^6 \pm 1 \times 10^4$ ($n = 3$); $2.15 \times 10^6 \pm 7 \times 10^3$ ($n = 3$) cells/mL for TOP, MID and BOT *inoculum*, respectively, after 36 h of incubation. The total amount of cells harvested differed significantly between BOT and the other two treatments after only 10 h of incubation (BOT > TOP-MID, Tukey’s *post hoc* test on ANOVA; $p_{\text{adj}} < 0.05$); while after 20 h all the treatments differed between each other (BOT > MID > TOP, Tukey’s *post hoc* test on ANOVA; $p_{\text{adj}} < 0.05$ per each pairwise comparison). Despite an apparent trend of specific growth rate increasing from TOP to BOT, only TOP’s specific growth rate was significantly lower than the other two treatments (Tukey’s *post hoc* test on ANOVA; $p_{\text{adj}} < 0.05$) (Figure 2(b)). A greater within-group variation was observed for the MID treatment.

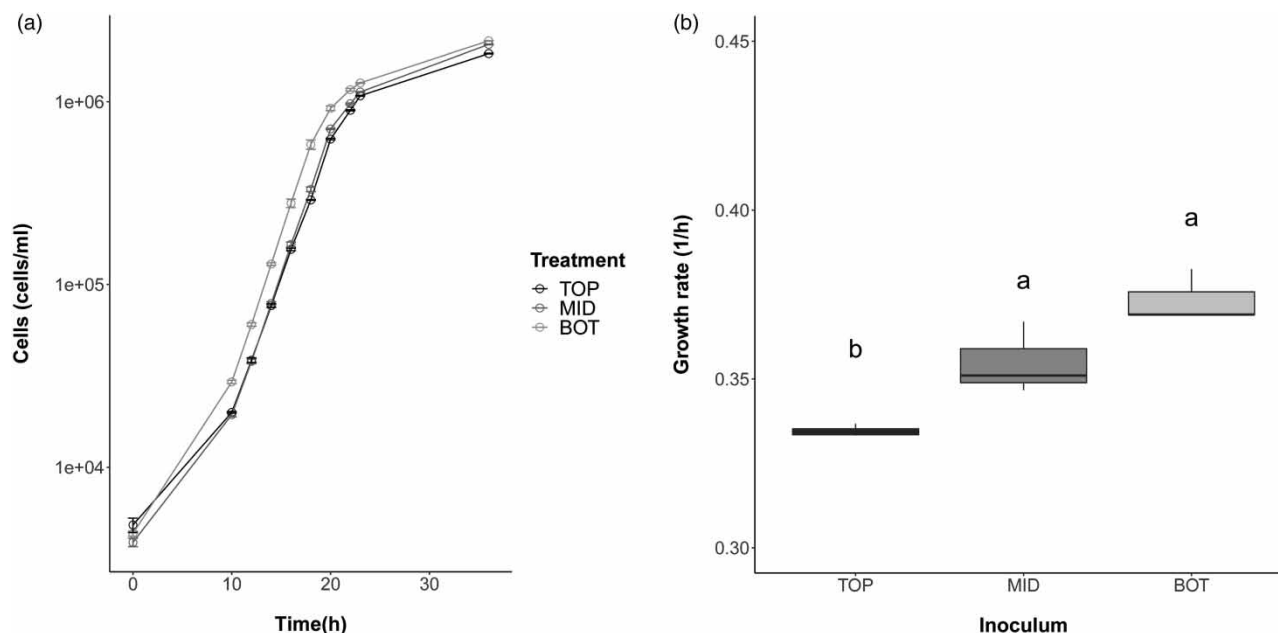


Figure 2 | Trends of cell abundances (a) and growth rates (b). Abundances were measured over the course of the experiment for the three treatments (mean \pm s.e., $n = 3$ replicates). Letters (a,b,c) in (a) denote significant differences between treatments with regard to cell abundances at the beginning of incubation (0 h) and after 10, 20 and 36 h assessed by Tukey's *post hoc* test on ANOVA. Letters (a,b) in (b) denote significant differences with regard to growth rates between treatments assessed by Tukey's *post hoc* test on ANOVA. Same letters denote no significant difference, different letters denote significant differences between treatments.

Microbial community structure

A total of 180,300 high-quality reads were obtained through sequencing, and 1,127 ASVs were detected in this study. Of these, 166 were shared between the three communities (Figure 3(b)); 305 were only found in the TOP, 199 only in the MID and 190 only present in the BOT. The remaining 267 ASVs were either shared between TOP-MID (81), or TOP-BOT (58) or MID-BOT (128). In terms of alpha biodiversity, the TOP community had the highest observed Richness, Shannon and Fisher Alpha indexes compared to BOT and MID communities (Table 2). The genera *Ralstonia* and *Pandora* were the most abundant in all the three communities accounting for 62 and 15% of the TOP community: 66 and 16% of the MID community and 62 and 16% of the BOT community, respectively.

The lineage *betI-B* of *Burkholderiales* and the genus *Curvibacter* were one to two orders of magnitude more abundant in the BOT and MID community (11 and 1% for BOT; 7% and 0.6% for MID) than in the TOP one (0.08% and 0.01%). The Genus *Sphingobium* and the lineage *alfIV alfIV-B* of *Sphingomonadales* were highly abundant in the TOP (5 and 8%, respectively), but almost absent in the other two treatments (0.0% and 0.002% for BOT; 0.003% and 0.0% for MID) (Figure 3(a)).

DOC concentration

DOC concentration before inoculation was 12.19 ± 0.04 mgC/L ($n = 3$); after 23 h of incubation, 12.35 ± 0.04 , 12.34 ± 0.04 , 12.18 ± 0.08 mgC/L were measured in the TOP, MID and BOT treatments, respectively. Only the TOP DOC was statistically different from T0 (Dunn's *post hoc* test on Kruskal-Wallis *H* test; $p_{\text{adj}} < 0.05$), but no significant difference between final DOC treatments was observed (Figure 4). Again, within-group variation was noticeable, especially for the TOP and BOT treatments.

DOM degradation

The initial DOC was mainly composed of humic substances ($83 \pm 0.4\%$), but the compound groups BB ($8.0 \pm 0.2\%$), LMWN ($5.7 \pm 0.2\%$), LMWA ($0.1 \pm 0.02\%$), and BP ($3.3 \pm 0.73\%$) were also found. This DOM composition changed slightly in all the samples during the incubation period. While no significant differences were observed among the three treatments at the end of the experiment regarding the different DOM fractions concentrations (Dunn's *post hoc* test on Kruskal-Wallis *H* test; $p_{\text{adj}} < 0.05$), significant differences were observed between T0 and the three treatments after 23 h incubation.

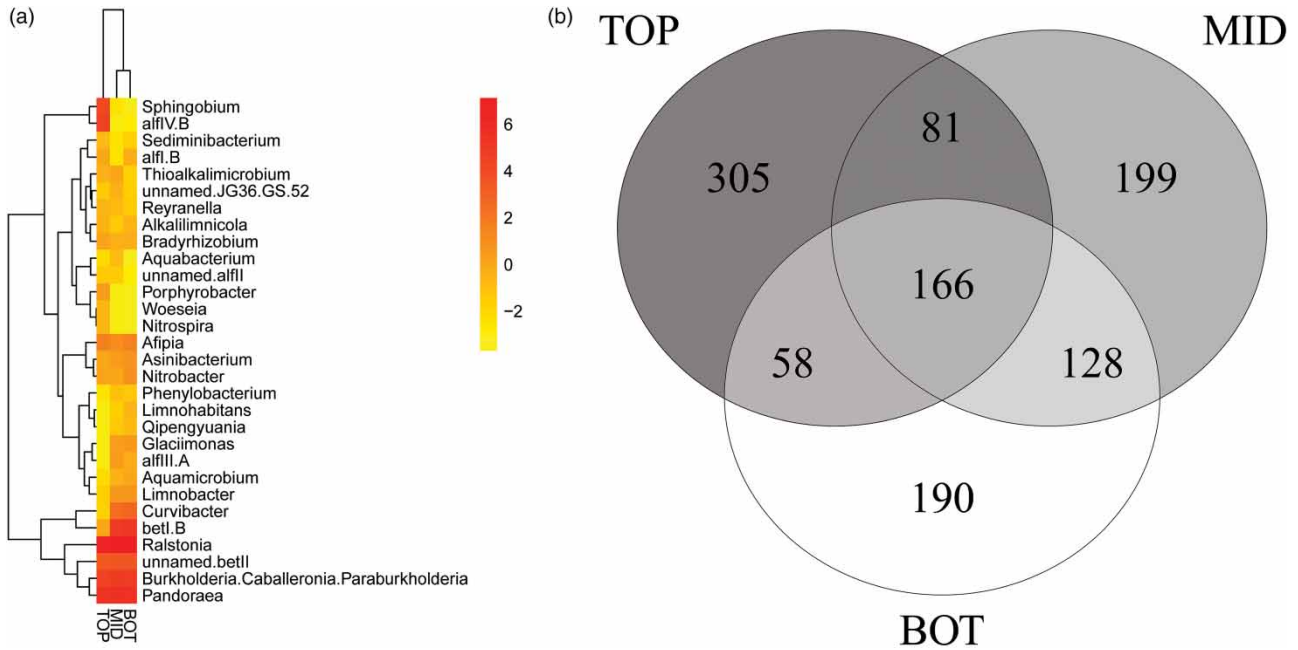


Figure 3 | Heatmap of the communities in the three treatments at genus level with both rows and columns ordered using hierarchical (average linkage) clustering (a). Venn diagram of the ASVs found in the treatments (b).

Table 2 | Alpha diversity parameters for the pooled triplicates

Sample	Number of high-quality reads	Richness	Fisher Alpha	Shannon
TOP	53,948	610	96	4.13
MID	71,954	547	85	3.99
BOT	54,398	541	84	4.10

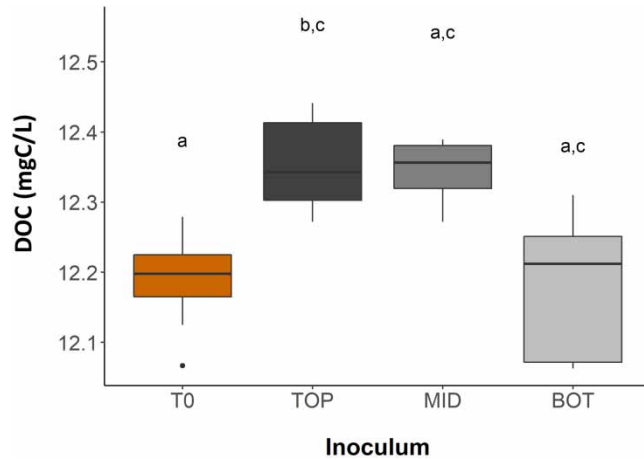


Figure 4 | Boxplot of the DOC concentration at $T = 0$ and the three treatments (TOP, MID, BOT) after 23 h incubation. Letters (a,b,c) denote significant differences with regard to DOC concentration in the different treatments assessed by Dunn’s *post hoc* test on Kruskal–Wallis H test. Same letters denote no significant difference, different letters denote significant differences between treatments.

Although no reduction in HS (Figure 5(a)) concentration was observed in TOP and MID from T0 to T23, BOT exhibited a significant decrease in HS content compared to T0 and significant increase in both BB content and molecularity (Figure 5(c)).

Throughout incubation, the LMWN carbon fraction did not change (Figure 6(a)). The LMWA concentration, on the other hand, decreased in the TOP and MID treatments. However, the difference between T0 and T23 was only statistically

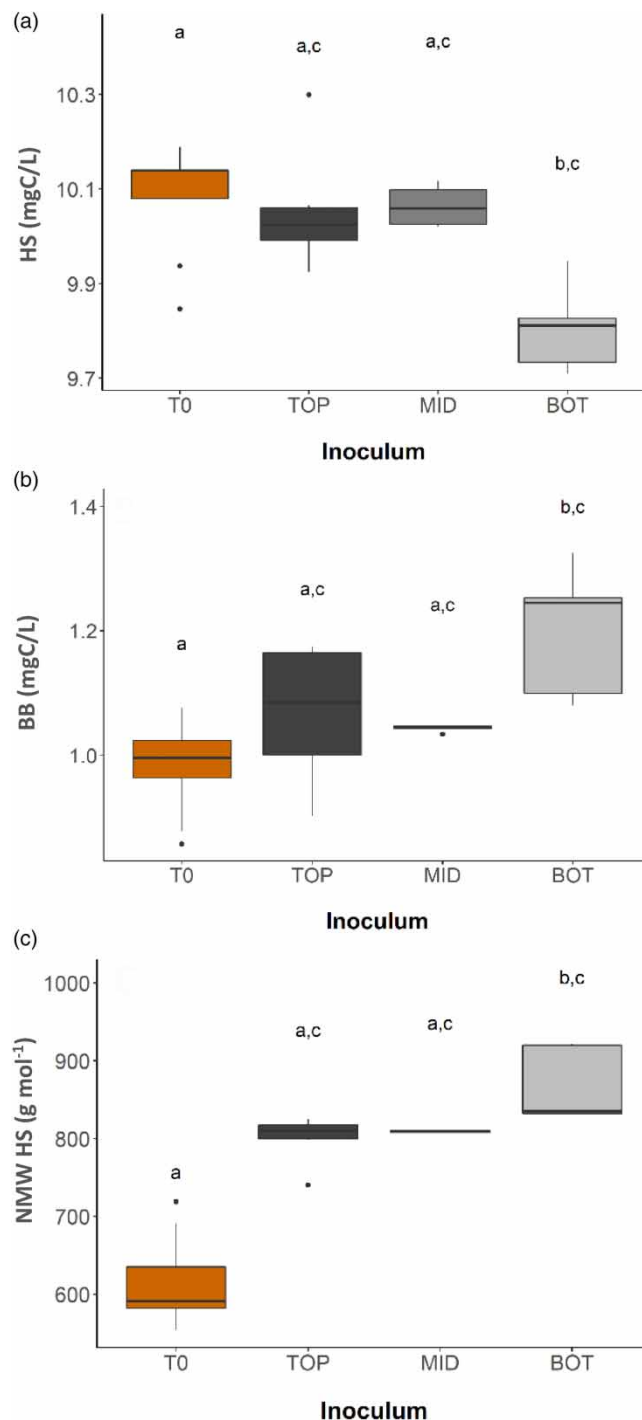


Figure 5 | Boxplots of HS concentration (a), BB concentration (b), and molecularity of the HS pool (c) at $T=0$ and in the three treatments (TOP, MID, BOT) at $T=23$. Letters (a,b,c) in a, b, and c denote significant differences in concentration between the different treatments assessed by Dunn's *post hoc* test on Kruskal–Wallis H test. Same letters denote no significant difference, different letters denote significant differences between treatments.

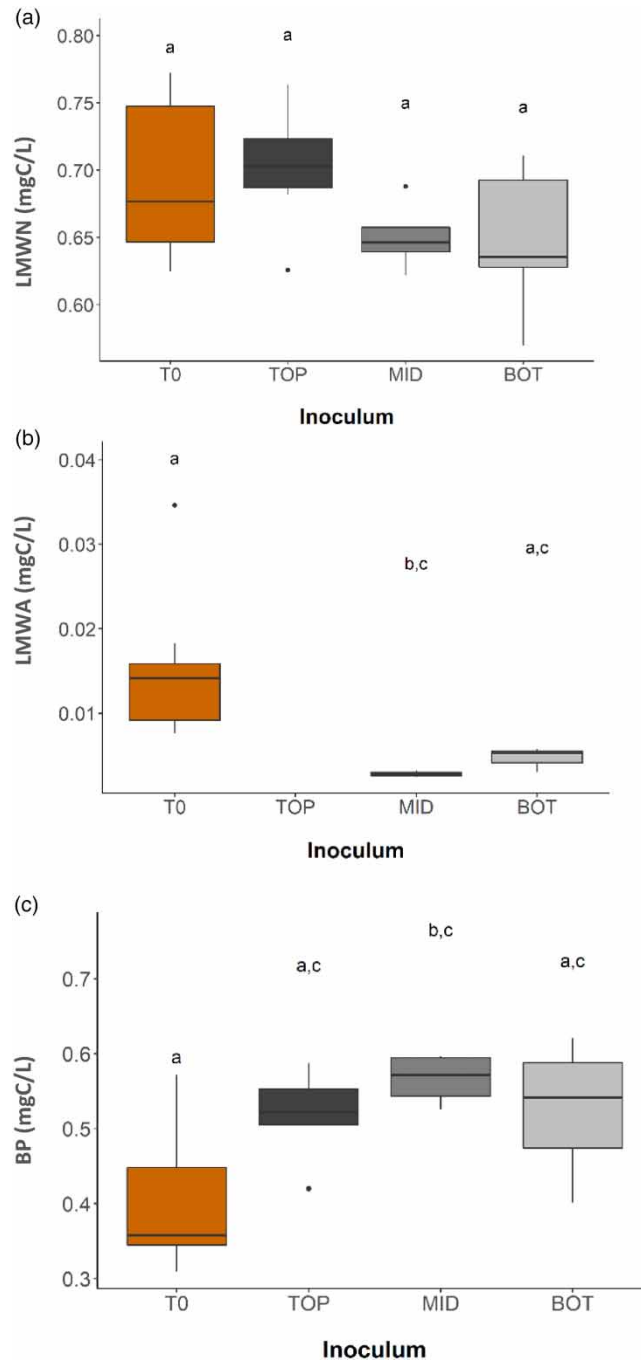


Figure 6 | Boxplots of the LMWN (a), LMWA (b), and BP (c) at $T = 0$ and (TOP, MID, and BOT) at $T = 23$ h. Letters (a,b,c) in a, b, and c denote significant differences in concentration between the different treatments assessed by Dunn's *post hoc* test on Kruskal–Wallis H test. Same letters denote no significant difference, different letters denote significant differences between treatments.

significant for MID (Dunn's *post hoc* test on Kruskal–Wallis H test; $p_{\text{adj}} < 0.05$); the concentration of LMWA in TOP fell below the LOD (Figure 6(b)). Finally, the BP concentration increased significantly only in MID at the end of the experiment (Dunn's *post hoc* test on Kruskal–Wallis H test; $p_{\text{adj}} < 0.05$) (Figure 6(c)). T0 showed a larger variance, while TOP had a significant outlier.

DISCUSSION

The aim of this study was to explore the ability of microbial communities extracted from different depths of a biofilter to degrade DOM fractions. Understanding this is essential to improve biofilter performances and DOM removal in drinking water treatments.

First, our results showed that the microbial communities enriched from three different depths of a biofilter (extracted and transformed into three *inocula*: TOP, MID, BOT) varied in their growth rate. While they were exposed to the same DOM composition and incubated under the same controlled conditions, the MID and BOT communities showed faster growth rates than the TOP and, consequently, a higher abundance of cells at the end of the experiment. Although a difference between MID and BOT growth rates was detectable (Figure 2(b)), it was not statistically significant ($P > 0.05$). This outcome is highly likely a result of high within-group variation of MID treatment presented by the wider error of the boxplot.

Assuming an average content of organic carbon per cell equal to 1.5×10^{-13} g of C/cell (as suggested by Vrede *et al.* (2002) and Pick *et al.* (2019)), the total net growth of cells at the end of the 23 h incubation accounted for the 1.31% and 1.36% of the total initial DOC content in the TOP and MID treatment, respectively, and for the 1.53% of the BOT treatment. Therefore, we expected to see a similar percentage decrease in the DOC concentration values; however, we did not observe a decrease in DOC concentration for any of the treatments. The expected change in DOC concentration might have fallen within the instrument's error.

Our results showed that the three microbial communities differed in the type of DOM compound group utilised during the incubation process. This assumes that the change in DOM distribution at the end of the incubation reflects the utilisation of DOM fractions (as identified by the LC-OCD-UVD-OND) by the three different communities. The TOP and MID treatments removed compounds belonging to the fraction of DOM with a low molecular weight – LMWA (Figure 6(b)). The BOT community, on the other hand, used the complex and the most abundant fraction of HS (Figure 5(a)). The metabolism of the different DOM fractions by heterotrophic bacteria is a complex and controversial subject (Amon & Benner 1996). The traditional view is that small molecules present in the DOM pool (up to ~600 Da) are also the most labile (Weiss *et al.* 1991), since they can be readily taken up by microorganisms across their cell membrane, and they are the C-source preferentially chosen by microorganisms (Münster & Chróst 1990). Bigger and more complex molecules (greater than 600 Da) would require extracellular enzymes for the conversion into smaller and more easily degradable compounds; therefore, they are considered more recalcitrant to microbial activity. Although biologically more recalcitrant than LMWA and LMWN, several studies have shown that a portion of humic substances is biologically degradable; this has been observed both in natural (Moran & Hodson 1990; Volk *et al.* 1997), and engineered environments (Hammes *et al.* 2011; Lautenschlager *et al.* 2014). The HS fraction was the most abundant DOM fraction in our experiment, accounting for 82.7% of the total dissolved organic carbon present in water. The high concentration of such compounds in freshwater compensates for their slower rates of utilisation (Volk *et al.* 1997). Our results suggest that only BOT was able to degrade the widely abundant HS fractions, which could explain the higher growth rate observed in the BOT community, as compared to TOP and MID.

Along with a decrease of HS in BOT treatment, we also observed an increase in its molecularity. On the other hand, the TOP and MID treatments demonstrated no removal of HS and no change in the molecularity of the HS pool. The detailed composition of the HS structure is unknown. However, it has been suggested that they are composed of low-molecular-weight compounds weakly attached to a larger refractory core (Gerke 2018; Finkbeiner *et al.* 2020). The BOT community showed microbial degradation of the HS fraction as suggested by the significant decrease in its concentration. However, it seems that only the small HS molecules were degraded by microorganisms since a decrease of the HS concentration fraction corresponded to an increase of its molecularity. The microbial activity in the BOT treatment removed the small HS molecules leaving the big ones in the DOM pool.

Our study reports no removal of the LMWN and BB, although these fractions are generally considered microbially labile and their biological removal has been reported in several studies (Boon *et al.* 2011; Krzeminski *et al.* 2019). However, these studies used ozonated waters, in which DOM is oxidised and broken down into smaller (more bioavailable) components. In our study, we used non-ozonated surface water where these compounds are presumed to be more refractory to biological degradation (Amon & Benner 1996; Vasyukova *et al.* 2014; Chen *et al.* 2016). The refractory nature of BB as well as the fact that BB are the product of HS breakdown (Huber *et al.* 2011), caused the BB concentration to increase in the BOT treatment during incubation. Our study also reports no removal of BP while these fractions are generally considered easily available for microbial degradation (Vasyukova *et al.* 2014; Chen *et al.* 2016). On the contrary, here we observed an increase

in the BP concentrations during incubation in all treatments, with only the MID treatment being statistically significant (due to high variances). BP could have been formed by the microbial cells during their growth. Lautenschlager *et al.* (2014) also observed a slight increase of the BP concentrations in their reservoir with treated drinking water, where the presence of cells was also reported.

The three treatment communities also showed different compositions, with TOP sharing the lowest similarity with the other two. The structure of a microbial community impacts its ability to degrade the different DOM fractions (Logue *et al.* 2016). While the degradation of low-molecular-weight DOM is believed to be a functional trait common to many microbial communities, the ability to utilise more recalcitrant DOM (such as HS and BP with greater molecular weight) is considered a trait less widely distributed (Logue *et al.* 2016), which would require either that the microbes in the community act in concert with each other or the presence of key taxa capable of facilitating the overall degradation process. Therefore, the different structure of the three communities might have influenced their ability to degrade the DOM pool, with the BOT community possessing the rarer ability to degrade complex organic carbon molecules such as the HS fraction. The genus *Curvibacter*, which was more abundant in the BOT and MID communities, has been thought to play an important role in the DOM degradation of freshwater since it seems to possess the ability to utilise specific types of carbon source (Wu *et al.* 2018). Hence, our results seem to suggest that some of the taxa in the *Curvibacter* genus could play an important role in the degradation of the HS fraction, which was significant in the BOT treatment. However, it is unclear why we did not observe a similar reduction in the MID community. The short duration of our experiment (hours vs days), compared to others (Logue *et al.* 2016; Wu *et al.* 2018) could also explain the lack of more significant differences between the treatments. However, it is important to acknowledge that the duration of our experiment (23 h) exceeded both the Empty Bed Contact Time (EBCT) (7.5 h) of the laboratory-scale biofilter that generated the communities and the average EBCT of full-scale biofilters (which ranges between few minutes for rapid gravity filters to a few hours for slow sand filters). Choosing longer incubation times would have enabled us to observe the degradation of more complex organic carbon compounds (Wu *et al.* 2018) and assess microbial succession; however these mechanisms are unlikely to occur within the timeframe operation of a biofilter.

Our experimental findings provide additional confirmation that microbial communities developed at different depths of a biofilter exhibit distinct abilities to degrade DOM fractions, as previously observed by Boon *et al.* However, our study goes beyond the findings of Boon *et al.* by explicitly demonstrating that these differences can be attributed to the specific microbial communities present at each depth since this was the only factor differing among treatments in our experiment. This could only be suggested in Boon's work. Indeed, Boon *et al.* identified residual ozone at the top of the filters as an additional co-factor potentially influencing the observed differences.

The extent to which our results can be interpreted as a generalised model of DOM degradation in biofilters is limited. We acknowledge the fact that for our study, we did not employ the original biofilter communities, but enriched *inocula* instead. However, the original biofilter communities showed a distinct separation in terms of composition and diversity from top to bottom (Supplementary material, Figure S1). Therefore, we can assume that the differences observed in the three *inocula*'s abilities to degrade DOM, as well as their composition studied after 36 h of incubation, are the consequence of the initial compositional difference of the biofilter communities from which they were derived (Logue *et al.* 2016). We can speculate that such differences are a consequence of the adaptation of the original biofilter communities to the different environmental niches developing at different depths of a biofilter (as also suggested by Boon *et al.* (2011)) and that lower depths might select for communities capable of degrading more complex DOM compounds. However, whether this results from their continued exposure to such DOM compound groups during the biofilter operation needs further investigation.

CONCLUSIONS

We have shown that microbial communities from different depths of the biofilter had different patterns of DOM utilisation with the bottom communities growing fastest, preferring different DOM fractions, and showing significantly different community compositions. We speculated that such differences resulted from the adaptation of the original biofilter communities to the environmental niches developing at different depths of a biofilter and that lower depths might select for communities capable of degrading more complex DOM compounds. While our experiment provides valuable initial understanding, further studies are needed to explore the relationship between microbial communities at different depths of a biofilter and their specific abilities to degrade DOM fractions. Future work should be conducted on the original biofilter communities and

should employ comprehensive analytical approaches beyond 16S rRNA sequencing. Techniques such as metagenomics or metabolomics would provide deeper insights into the functional potential and metabolic pathways of these microbial communities which is essential to identify and understand the underlying mechanisms driving the degradation of DOM fractions within biofilters. This comprehensive approach will enhance our knowledge of the intricate interplay between microbial communities and DOM processing, ultimately improving the design and optimisation of biofilter systems for efficient water treatment.

FUNDING

This work is supported by Royal Academy of Engineering-Scottish Water Research Chair (RCSRF171864); M.V. was supported by the Royal Academy of Engineering under the Research Fellowship scheme (RF\201819\18\198); U.Z.I. is supported by NERC, UK, NE/L011956/1. R.P. acknowledges financial support to the European Research Council BOOGIE project under the European Union's Horizon 2020 research and innovation programme (grant number 949495). W.S. acknowledges financial support from the Engineering and Physical Sciences Research Council for the Decentralised Water Technologies project (EPSCR/V030515/1).

DATA AVAILABILITY STATEMENT

All relevant data are included in the paper or its Supplementary Information. The raw sequence files supporting the results of this article are available in the European Nucleotide Archive under the project accession number **PRJEB64260**.

CONFLICT OF INTEREST

The authors declare there is no conflict.

REFERENCES

- Amon, R. M. W. & Benner, R. 1996 Bacterial utilization of different size classes of dissolved organic matter. *Limnol. Oceanogr.* **41** (1), 41–51. <https://doi.org/10.4319/lo.1996.41.1.0041>.
- Baghoth, S. A., Sharma, S. K., Guitard, M., Heim, V., Croué, J. & Amy, G. L. 2011 Removal of NOM-constituents as characterized by LC-OCD and F-EEM during drinking water treatment. 412–424. <https://doi.org/10.2166/aqua.2011.059>.
- Bai, Y. H., Liu, R. P., Liang, J. S. & Qu, J. H. 2013 Integrated metagenomic and physiochemical analyses to evaluate the potential role of microbes in the sand filter of a drinking water treatment system. *PLoS One* **8** (4), e61011. <https://doi.org/ARTN e61011>. doi:10.1371/journal.pone.0061011.
- Basu, O. D., Dhawan, S. & Black, K. 2016 Applications of biofiltration in drinking water treatment – a review. *J. Chem. Technol. Biotechnol.* **91** (3), 585–595. <https://doi.org/10.1002/jctb.4860>.
- Boon, N., Pycke, B. F. G., Marzorati, M. & Hammes, F. 2011 Nutrient gradients in a granular activated carbon biofilter drives bacterial community organization and dynamics. *Water Res.* **45** (19), 6355–6361. <https://doi.org/10.1016/j.watres.2011.09.016>.
- Broman, E., Asmala, E., Carstensen, J., Pinhassi, J. & Dopson, M. 2019 Distinct coastal microbiome populations associated with autochthonous- and allochthonous-like dissolved organic matter. *Front. Microbiol.* **10** (November), 1–15. <https://doi.org/10.3389/fmicb.2019.02579>.
- Caporaso, J. G., Kuczynski, J., Stombaugh, J., Bittinger, K., Bushman, F. D., Costello, E. K., Fierer, N., Peña, A. G., Goodrich, J. K., Gordon, J. I., Huttley, G. A., Kelley, S. T., Knights, D., Koenig, J. E., Ley, R. E., Lozupone, C. A., McDonald, D., Muegge, B. D., Pirrung, M., Reeder, J., Sevinsky, J. R., Turnbaugh, P. J., Walters, W. A., Widmann, J., Yatsunenko, T., Zaneveld, J. & Knight, R. 2010 QIIME allows analysis of high-throughput community sequencing data. *Nat. Methods* **7** (5), 335–336. <https://doi.org/10.1038/nmeth.f.303>.
- Chen, F., Peldszus, S., Elhadidy, A. M., Legge, R. L., Van Dyke, M. I. & Huck, P. M. 2016 Kinetics of natural organic matter (NOM) removal during drinking water biofiltration using different NOM characterization approaches. *Water Res.* **104**, 361–370. <https://doi.org/10.1016/j.watres.2016.08.028>.
- Chen, Q., Lønborg, C., Chen, F., Gonsior, M., Li, Y., Cai, R., He, C., Chen, J., Wang, Y., Shi, Q., Jiao, N. & Zheng, Q. 2022 Increased microbial and substrate complexity result in higher molecular diversity of the dissolved organic matter pool. *Limnol. Oceanogr.* **67** (11), 2360–2373. <https://doi.org/10.1002/lno.12206>.
- Cottrell, M. T. & Kirchman, D. L. 2000 Natural assemblages of marine proteobacteria and members of the cytophaga-flavobacter cluster consuming Low- and high-Molecular-Weight dissolved organic matter. *Appl. Environ. Microbiol.* **66** (4), 1692–1697. <https://doi.org/10.1128/AEM.66.4.1692-1697.2000>.
- Finkbeiner, P., Moore, G., Pereira, R., Jefferson, B. & Jarvis, P. 2020 The combined influence of hydrophobicity, charge and molecular weight on natural organic matter removal by ion exchange and coagulation. *Chemosphere* **238**, 124633. <https://doi.org/10.1016/j.chemosphere.2019.124633>.

- Gang, D., Clevenger, T. E. & Banerji, S. K. 2003 Relationship of chlorine decay and THMs formation to NOM size. *J. Hazard. Mater.* **96** (1), 1–12. [https://doi.org/10.1016/S0304-3894\(02\)00164-4](https://doi.org/10.1016/S0304-3894(02)00164-4).
- Gerke, J. 2018 Concepts and misconceptions of humic substances as the stable part of soil organic matter: a review. *Agronomy*. <https://doi.org/10.3390/agronomy8050076>.
- Hammes, F. a. & Egli, T. 2005 New method for assimilable organic carbon determination using flow-cytometric enumeration and a natural microbial consortium as inoculum. *Environ. Sci. Technol.* **39** (9), 3289–3294. <https://doi.org/10.1021/es048277c>.
- Hammes, F., Berney, M., Wang, Y. Y., Vital, M., Koster, O. & Egli, T. 2008 Flow-cytometric total bacterial cell counts as a descriptive microbiological parameter for drinking water treatment processes. *Water Res.* **42** (1–2), 269–277. <https://doi.org/DOI 10.1016/j.watres.2007.07.009>.
- Hammes, F., Boon, N., Vital, M., Ross, P., Magic-Knezev, A. & Dignum, M. 2011 Bacterial colonization of pellet softening reactors used during drinking water treatment. *Appl. Environ. Microbiol.* **77** (3), 1041–1048. <https://doi.org/10.1128/AEM.02068-10>.
- Hu, W., Liang, J., Ju, F., Wang, Q., Liu, R., Bai, Y., Liu, H. & Qu, J. 2020 Metagenomics unravels differential microbiome composition and metabolic potential in rapid sand filters purifying surface water versus groundwater. *Environ. Sci. Technol.* **54** (8), 5197–5206. <https://doi.org/10.1021/acs.est.9b07143>.
- Huber, S. A., Balz, A., Abert, M. & Pronk, W. 2011 Characterisation of aquatic humic and non-humic matter with size-exclusion chromatography – organic carbon detection – organic nitrogen detection (LC-OCD-OND). *Water Res.* **45** (2), 879–885. <https://doi.org/10.1016/j.watres.2010.09.023>.
- Krzeminski, P., Vogelsang, C., Meyn, T., Köhler, S. J., Poutanen, H., de Wit, H. A. & Uhl, W. 2019 Natural organic matter fractions and their removal in full-scale drinking water treatment under cold climate conditions in nordic capitals. *J. Environ. Manage.* **241** (January), 427–438. <https://doi.org/10.1016/j.jenvman.2019.02.024>.
- Lautenschlager, K., Hwang, C., Ling, F., Liu, W.-T., Boon, N., Köster, O., Egli, T. & Hammes, F. 2014 Abundance and composition of indigenous bacterial communities in a multi-step biofiltration-based drinking water treatment plant. *Water Res.* **62**, 40–52. <https://doi.org/10.1016/j.watres.2014.05.035>.
- Lechevallier, M. W., Shaw, N. E., Kaplan, L. A. & Bott, T. L. 1993 Development of a rapid assimilable organic carbon method for water development of a rapid assimilable organic carbon method for water. *Water. Appl. Environ. Microbiol.* **59** (5), 1526–1531.
- Leenheer, J. J. a. & Croué, J. J.-P. 2003 Characterizing aquatic dissolved organic matter. *Environ. Sci. Technol.* **37** (1), 18A–26A. <https://doi.org/10.1021/es032333c>.
- Logue, J. B., Stedmon, C. A., Kellerman, A. M., Nielsen, N. J., Andersson, A. F., Laudon, H., Lindström, E. S. & Kritzberg, E. S. 2016 Experimental insights into the importance of aquatic bacterial community composition to the degradation of dissolved organic matter. *ISME J.* **10** (3), 533–545. <https://doi.org/10.1038/ismej.2015.131>.
- Matilainen, A., Gjessing, E. T., Lahtinen, T., Hed, L., Bhatnagar, A. & Sillanpää, M. 2011 An overview of the methods used in the characterisation of Natural Organic Matter (NOM) in relation to drinking water treatment. *Chemosphere* **83** (11), 1431–1442. <https://doi.org/10.1016/j.chemosphere.2011.01.018>.
- Moona, N., Holmes, A., Wünsch, U. J., Pettersson, T. J. R. & Murphy, K. R. 2021 Full-Scale manipulation of the empty Bed contact time to optimize dissolved organic matter removal by drinking water biofilters. *ACS EST Water* **1** (5), 1117–1126. <https://doi.org/10.1021/acsestwater.0c00105>.
- Moran, M. A. & Hodson, R. E. 1990 Bacterial production on humic and nonhumic components of dissolved organic carbon. *Limnol. Oceanogr.* **35** (8), 1744–1756. <https://doi.org/10.4319/lo.1990.35.8.1744>.
- Münster, U. & Chróst, R. J. 1990 Origin, composition, and microbial utilization of dissolved organic matter. *May 2014*, 8–46. https://doi.org/10.1007/978-1-4612-3382-4_2.
- Oh, S., Hammes, F. & Liu, W.-T. 2018 Metagenomic characterization of biofilter microbial communities in a full-scale drinking water treatment plant. *Water Res.* **128**, 278–285. <https://doi.org/10.1016/j.watres.2017.10.054>.
- Palomo, A., Jane Fowler, S., Gülay, A., Rasmussen, S., Sichert-Ponten, T. & Smets, B. F. 2016 Metagenomic analysis of rapid gravity sand filter microbial communities suggests novel physiology of nitrospira Spp. *ISME J.* **10** (11), 2569–2581. <https://doi.org/10.1038/ismej.2016.63>.
- Peleato, N. M. N. M., McKie, M., Taylor-Edmonds, L., Andrews, S. A., Legge, R. L. & Andrews, R. C. 2016 Fluorescence spectroscopy for monitoring reduction of natural organic matter and halogenated furanone precursors by biofiltration. *Chemosphere* **153**, 155–161. <https://doi.org/10.1016/j.chemosphere.2016.03.018>.
- Pick, F. C., Fish, K. E., Biggs, C. A., Moses, J. P., Moore, G. & Boxall, J. B. 2019 Application of enhanced assimilable organic carbon method across operational drinking water systems. *PLoS One* **14** (12), 1–24. <https://doi.org/10.1371/journal.pone.0225477>.
- Pinto, A. J., Xi, C. & Raskin, L. 2012 Bacterial community structure in the drinking water microbiome is governed by filtration processes. *Environ. Sci. Technol.* **46** (16), 8851–8859. <https://doi.org/10.1021/es302042t>.
- Prévost, M., Rompré, A., Coallier, J., Servais, P., Laurent, P., Clément, B. & Lafrance, P. 1998 Suspended bacterial biomass and activity in full-scale drinking water distribution systems: impact of water treatment. *Water Res.* **32** (5), 1393–1406. [https://doi.org/10.1016/S0043-1354\(97\)00388-6](https://doi.org/10.1016/S0043-1354(97)00388-6).
- Rocker, D., Brinkhoff, T., Grüner, N., Dogs, M. & Simon, M. 2012 Composition of humic acid-degrading estuarine and marine bacterial communities. *FEMS Microbiol. Ecol.* **80** (1), 45–63. <https://doi.org/10.1111/j.1574-6941.2011.01269.x>.

- Rohart, F., Gautier, B., Singh, A. & Lê Cao, K. A. 2017 Mixomics: an R package for 'omics feature selection and multiple data integration. *PLoS Comput. Biol.* **13** (11), 1–19. <https://doi.org/10.1371/journal.pcbi.1005752>.
- Terry, L. G. & Summers, R. S. 2018 Biodegradable organic matter and rapid-rate biofilter performance: a review. *Water Res.* **128**, 234–245. <https://doi.org/10.1016/j.watres.2017.09.048>.
- Urfer, D., Huck, P. M., Booth, S. D. J. & Coffey, B. M. 1997 Biological filtration for BOM and particle removal: a critical review: the authors review key parameters and engineering variables influencing biological filtration and identify areas requiring further research. *J./Am. Water Work. Assoc.* **89** (12), 83–98. <https://doi.org/10.1002/j.1551-8833.1997.tb08342.x>.
- Vannote, R. L., Minshall, G. W., Cummins, K. W., Sedell, J. R. & Cushing, C. E. 1980 The river continuum concept. *Can. J. Fish. Aquat. Sci.* **37** (1), 130–137. <https://doi.org/10.1139/f80-017>.
- Vasyukova, E., Proft, R. & Uhl, W. 2014 Evaluation of dissolved organic matter fractions removal due to biodegradation. *Prog. Slow Sand Altern. Biofiltration Process. Furth. Dev. Appl.* **March 2021**, 59–66.
- Velten, S., Knappe, D. R. U., Traber, J., Kaiser, H. P., von Gunten, U., Boller, M. & Meylan, S. 2011 Characterization of natural organic matter adsorption in granular activated carbon adsorbers. *Water Res.* **45** (13), 3951–3959. <https://doi.org/10.1016/j.watres.2011.04.047>.
- Vignola, M., Werner, D., Wade, M. J., Meynet, P. & Davenport, R. J. 2018 Medium shapes the microbial community of water filters with implications for effluent quality. *Water Res.* **129**, 499–508. <https://doi.org/10.1016/j.watres.2017.09.042>.
- Volk, C. J., Volk, C. B. & Kaplan, L. A. 1997 Chemical composition of biodegradable dissolved organic matter in streamwater. *Limnol. Oceanogr.* **42** (1), 39–44. <https://doi.org/10.4319/lo.1997.42.1.0039>.
- Vrede, K., Heldal, M., Norland, S. & Bratbak, G. 2002 Elemental composition (C, N, P) and cell volume of exponentially growing and nutrient-limited bacterioplankton. *Appl. Environ. Microbiol.* **68** (6), 2965–2971. <https://doi.org/10.1128/AEM.68.6.2965-2971.2002>.
- Weiss, M., Abele, U., Weckesser, J., Welte, W., Schiltz, E. & Schulz, G. 1991 Molecular architecture and electrostatic properties of a bacterial porin. *Science (80-.)* **254**, 1627–1630. <https://doi.org/10.2307/3171302>.
- Wu, X., Wu, L., Liu, Y., Zhang, P., Li, Q., Zhou, J., Hess, N. J., Hazen, T. C., Yang, W. & Chakraborty, R. 2018 Microbial interactions with dissolved organic matter drive carbon dynamics and community succession. *Front. Microbiol.* **9** (JUN), 1234. <https://doi.org/10.3389/fmicb.2018.01234>.

First received 20 February 2023; accepted in revised form 10 July 2023. Available online 8 September 2023